C.P. No. 875

MINISTRY OF AVIATION

AERONAUTICAL RESEARCH COUNCIL

CURRENT PAPERS

A Note on the Turbulent Uniform-Property Hydrodynamic Boundary Layer on a Smooth Impermeable Wall; Comparisons of Theory With Experiment

By

M. P. Escudier and D. B. Spalding

Imperial College

LONDON: HER MAJESTY'S STATIONERY OFFICE

1966

Price 5s. 6d. net

A Note on the Turbulent Uniform-Property Hydrodynamic Boundary Layer on a Smooth Impermeable Wall; Comparisons of Theory with Experiment

- By -
M. P. Escudier and D. B. Spalding,
Imperial College

C.P. No.875*

August, 1965

SUMMARY

The recent experimental data of Bradshaw and Ferriss[1] are compared with generalisations deduced from earlier data, in respect of the mixing-length distribution and the dissipation integral; the agreement is satisfactory.

Also presented is a preliminary theory of boundary-layer development, employing an empirical formula for the relation between the dissipation integral, the drag coefficient and the shape factor; the integral momentum and kinetic-energy equations are solved numerically. The predictions of this theory are compared, in respect of shape factor, with the experiments of Bradshaw and Ferriss and those of many other experimenters. The agreement is satisfactory except for large adverse pressure gradient, where divergences of both positive and negative sign are observed; the reasons for these divergences are discussed.

1. Introduction

Bradshaw and Ferriss[1] have recently published the results of a set of particularly careful and detailed measurements on turbulent boundary layers in adverse pressure gradients; specifically, they studied both: an equilibrium boundary layer; and one in which the adverse pressure gradient fell from a positive value upstream to zero downstream. As Bradshaw and Ferriss rightly remark, their data can be used to test the generality of prediction procedures for turbulent boundary layers; the test will be particularly significant for prediction procedures which have been adjusted to fit data for boundary layers in which the adverse pressure gradient increases in the streamwise direction.

The present authors are developing prediction procedures for turbulent boundary layers, and have accordingly made use of the opportunity provided by Ref. 1 ; the results of their study are contained in the present note; also provided are comparisons of prediction and experiment for a large number of other boundary layers. The latter comparisons are provided to give perspective to the study of the data of Ref. 1 .

The impression might be gained from the paper of Bradshaw and Ferriss that the boundary layers which they have studied differ greatly, from those investigated by earlier authors, in respect of the relations between the profiles of shear stress and velocity profile. In the present note we therefore make some comparisons which show that the similarities are at least as pronounced as the differences; it cannot indeed be said with certainty that the latter are not merely the result of experimental scatter.

2./

*Replaces A.R.C.27 302

2. The Relation Between Shear Stress and Velocity

In order to demonstrate the common features of the Bradshaw-Ferriss and other turbulent boundary layers, we make use, as a definition, of the Prandtl[2] mixing-length formula:

$$\ell \equiv \left\{ \frac{\tau}{\rho \left|\frac{\partial u}{\partial y}\right| \left(\frac{\partial u}{\partial y}\right)} \right\}^{\frac{1}{2}}, \qquad \ldots (1)$$

where ℓ is the mixing length,

τ is the shear stress,

ρ is the fluid density,

u is the (time-mean) velocity in the mainstream direction, and

y is the distance normal to the wall.

With the aid of this formula, $\ell(y)$ can obviously be evaluated from data for $\tau(y)$ and $u(y)$.

We choose to represent the $\ell(y)$ distributions resulting from our evaluations in dimensionless form; both ℓ and y have been divided by the y-value of the outer edge of the boundary layer, y_G. Thus:

$$\lambda \equiv \ell / y_G , \qquad \ldots (2)$$

$$\xi \equiv y / y_G . \qquad \ldots (3)$$

The values of y_G were determined by inspection of the reported velocity profiles, with an estimated accuracy of $\pm 5\%$.

The resulting mixing-length distributions across the boundary layers are shown in Fig.1*, which has been extracted from a wider survey by Escudier[3]. The curves represent the experimental data; the two straight lines, which are repeated in each graph to provide a base of reference, represent the formulae which have been used by the authors elsewhere as the foundation of a prediction procedure[4].

$$\left.\begin{aligned} 0 \leqslant \xi \leqslant \lambda_G/\kappa \;&:\; \lambda = \kappa \xi \;, \\ \lambda_G/\kappa < \xi \leqslant 1 \;&:\; \lambda = \lambda_G \;, \end{aligned}\right\} \qquad \ldots (4)$$

where the values 0·075 and 0·4 have been chosen for λ_G and κ respectively.

The data of Bradshaw and Ferriss appear in graphs (a) and (b) of Fig.1; evidently the $\lambda(\xi)$ profiles of these authors do not differ greatly among themselves; and they are not radically different from those of the other authors. Further data could have been taken from Ref. 3 to support the same trends.

When assessing the degree of similarity between the curves, it is helpful to remember:

(i) That the shear stress is proportional to the square of mixing length; so the $\lambda(\xi)$ representation tends to minimise the differences in the shear-stress-versus-velocity relation;

(ii)/

---

*A list of all figures, with brief descriptions, is given on page 14.

(ii) That where ξ lies between 0·8 and 1·0, although the mixing length tends to rise rapidly and the differences between the profiles may be great, the velocity gradients are small; consequently the shear stresses are small and errors in λ are of slight importance;

(iii) The values of λ rest on determinations of the slope of the velocity profile; the inevitable experimental error thus introduces a large scatter in the $\lambda(\xi)$ curves. In this respect therefore the method of plotting magnifies the differences between boundary layers.

Fig. 1 is the first piece of evidence which we put forward for the similarity between the Bradshaw-Ferriss boundary layers and those studied by earlier authors.

3. The Dissipation Integral

The method of boundary-layer prediction pioneered by Rotta[5] and Truckenbrodt[6], based on the integral momentum and kinetic-energy equations, requires knowledge of the dissipation integral $\bar{s}$, defined by:

$$\bar{s} \equiv \frac{1}{\rho_G u_G^3} \int_0^{y_G} \tau \frac{\partial u}{\partial y} \, dy \quad . \qquad \ldots (5)$$

Here ρ_G and u_G are respectively the density and velocity of the main stream. The quantity $\bar{s}$ is sometimes represented symbolically by: $(d_1 + t_1)/(\rho U^3)$.

As has been shown elsewhere, the particular recommendations for the $\bar{s}$ function made in Refs. 5 and 6 are valid only in very restricted circumstances; better ones can be based on the mixing-length profile of equation (4) and on suitable velocity-profile assumptions[4]. Here however we draw attention to an empirical formula derived by the present authors from a least-squares analysis of shear-stress data, measured with hot-wire equipment in a variety of boundary-layer situations by: Bradshaw and Ferriss[1], Klebanoff[7], Moses[8], Newman[9], Sandborn and Slogar[10], and Schubauer and Klebanoff[11].

The formula is:

$$\bar{s} = 0{\cdot}547 \left(\frac{c_f}{2} \right) + 10^{-3}(2{\cdot}107H - 2{\cdot}286) \quad , \qquad \ldots (6)$$

where c_f is the local drag coefficient, and H is the shape factor (displacement thickness divided by momentum thickness).

Fig. 2 displays the data from which equation (6) was derived. The plain dots represent the data of references 7 to 11 ; the encircled dots represent the data of Bradshaw and Ferriss[1]. Fig.2 gives little reason for believing that the latter data deviate radically from the former. The deviations that exist may be systematic; but they are of the order of a few tens per cent.

Fig.2 is the second item of evidence for the similarity between the data of reference 1 and those of other workers.

4./

4. The Prediction of the Development of Turbulent Boundary Layers

The present authors have investigated, among other methods* of predicting boundary-layer development on smooth impermeable walls when the density is uniform, the implications of the following set of assumptions:-

(i) The dissipation integral obeys equation (6);

(ii) The local drag coefficient is related to the Reynolds number and the shape factor by the well-known Ludwieg-Tillmann relation (12).

(iii) The shape factor H is related to the quantity H_3, representing the kinetic-energy thickness divided by the momentum thickness, by the formulae recommended by Nicoll and Escudier[13], namely:

$$2{\cdot}8 \geq H \geq 1{\cdot}25 \quad : \quad H_3 = 1{\cdot}431 - 0{\cdot}097/H + 0{\cdot}775/H^2 . \qquad \ldots (7)$$

The data from which this formula was deduced are shown in Fig.3.

Predictions have been made, by this means, for many of the experiments which can be found in the literature. The differential equations in question were integrated numerically, for the prescribed main-stream velocity distribution, and the predicted values of momentum thickness, shape factor, etc., were then compared with the reported values. The initial conditions of the integration were the experimental values of momentum thickness and shape factor; but otherwise no individual adjustments were made to improve the agreement between prediction and experiment.

Some of the results of the comparison are displayed in Fig.4, the shape factor H being the boundary-layer property selected for consideration. The abscissa is the length Reynolds number, R_x, defined by:

$$R_x \equiv \int_0^x (\rho_G u_G / \mu_G)\, dx , \qquad \ldots (8)$$

where x is the distance along the surface in the mainstream direction and μ_G is the fluid viscosity. The individual diagrams are distinguished by the names of the experimenters who reported the data; dots represent experimental values while curves represent predictions.

Inspection of the diagrams, with particular reference to the degree of agreement between prediction and experiment, seems to justify the following conclusions:-

(i) Apart from a few failures, the extent of agreement is generally satisfactory, at least when judged against the poor results reported in Thompson's recent survey[14] of the predictive ability of earlier theories.

(ii) The predictions for the two Bradshaw-Ferriss boundary layers are not notably better or worse than those for other experiments. (Incidentally, a complete failure to predict the H-variation for the first u_G-x variation reported in Ref. 1 , revealed that the reported u_G values were in error; the diagram marked "Bradshaw and Ferris 1" is based on corrected values, subsequently confirmed by those authors.)

The/

*For example, as was mentioned earlier, a procedure has been developed which is based on the mixing length formula (4)[4].

The second Bradshaw-Ferriss experiment, for the "recovering" boundary layer (H diminishing in the main-stream direction) is not the only one of its kind, as may be seen from Fig.4. For example, the experiments of Klebanoff and Diehl[15] are of this character; in their case the disturbance was a roughness element, distributed or local, upstream of a flat surface. Also two of the experiments of Moses[8] embody the recovery from the effects of an adverse pressure gradient; our theory predicts one of them satisfactorily; but the computation for the other was stopped when H attained the separation value of 3.

(iii) Although there are some fairly successful predictions of separation (e.g. Moses 2, Schubauer and Spangenberg[23] C, E and F), the failures are more numerous; most of these are such that H rose more rapidly than predicted.

(iv) On some cases, the disagreement between prediction and experiment may perhaps be more probably ascribed to the latter than the former. For example, the downstream H-values of experiments 1 and 2 of Klebanoff and Diehl seem implausibly high.

5. Discussion of Fig.4

The comparisons of theory with experiment in Fig.4 do not, of course, settle the question of whether it is possible to predict boundary-layer development with a theory which rests, as does the present one, on the assumption that the shear-stress profile is uniquely determined by the velocity profile; for no attempt has so far been made systematically to seek the $\bar{s}$ and c_f functions of H and Reynolds number which give the best predictions.

That the $\bar{s}$ function must be chosen with care can be recognised by writing the equation for dH/dx which follows from the momentum and kinetic-energy equations, namely:

$$\delta_2 \frac{dH}{dx} = \frac{dH}{dH_3} \left\{ 2\bar{s} - H_3 \left(\frac{c_f}{2} \right) + H_3 \, (H - 1) F_2 \right\}, \qquad \ldots (9)$$

where δ_2 stands for the momentum thickness, dH/dH_3 is a negative quantity varying somewhat with H, and:

$$F_2 \equiv \frac{\delta_2}{u_G} \frac{du_G}{dx} \, . \qquad \ldots (10)$$

Near separation, c_f is of course small and F_2 is negative, dH/dx is therefore proportional to the difference between the dissipation integral and the quantity $\frac{1}{2} H_3 (H - 1)(-F_2)$. Obviously, a 10% error in the $\bar{s}$ value may easily change dH/dx from a positive to a negative value when the two terms have about the same size. It is therefore not surprising, in view of the scatter displayed on Fig.2, and of the unsophisticated nature of equation (6), that predictions are sometimes in error when $-F_2$ is large.

When weighing this consideration, two points deserve particular attention. The first is that the aerodynamicist's interest in separation lies chiefly in preventing its occurrence; and engineering good practice demands that a safety factor should be incorporated in a design. For this purpose, the criterion is already quite clear; the quantity $-F_2$ should never be allowed to increase above (say) 0·002. The predictions of F_2 by the present authors are fortunately quite accurate.

The/

The second point is that there are many possible influences on the $\bar{s}$ function, the systematic exploration of which may lead to improved methods of prediction. Among these influences are: free-stream turbulence, the rate of enlargement of the boundary-layer thickness, the rate of change of the velocity profile, the convexity of the surface, and the local pressure gradient itself. If these influences exist at a significant level, research can disclose them; and, whether they require expression by algebraic equations or by differential ones, modern computing facilities are more than adequate for their incorporation in the prediction procedure.

6. Conclusions

It is the opinion of the present authors that the experimental results of Bradshaw and Ferriss[1] reveal a heartening similarity to exist between their boundary layers and those reported elsewhere in the literature. The near universality of the mixing-length distribution may form a valuable jumping-off point for theoretical studies.

The procedure outlined in Section 4 is fairly successful in predicting the development of the boundary-layer shape factor; but it is clearly not likely to be the optimum procedure, even among procedures of its own kind. The exploration of the factors influencing the dissipation integral is one of the most urgent topics of turbulent-boundary-layer research.

7. Acknowledgements

The authors' thanks are due to Mr. P. Bradshaw, Prof. F. H. Clauser, and Mr. W. Spangenberg for making available unpublished details of their experimental work. Thanks are also due to Mr. J. A. P. Stoddart for supplying tabulated information about the Ludwieg-Tillmann experiments.

List of Symbols/

List of Symbols

		Equation of first mention
$c_f/2$	Local drag coefficient	(6)
F_2	Pressure-gradient parameter	(9)
H, H_3	Boundary-layer shape factors	(6), (7)
ℓ	Prandtl mixing length	(1)
R_x	Length Reynolds number	(8)
$\bar{s}$	Dissipation integral	(5)
u	Velocity of fluid in mainstream direction	(1)
u_G	Value of u in mainstream	(5)
x	Distance along wall in mainstream direction	(8)
y	Distance from wall in direction towards the fluid	(1)
y_G	Value of y at the outer "edge" of the boundary layer	(2)
δ_2	Boundary-layer momentum thickness	(9)
$\varkappa$	Constant appearing in mixing-length distribution near the wall	(4)
λ	Non-dimensional mixing length	(2)
λ_G	Value of λ in outer region of boundary layer	(4)
μ_G	Dynamic viscosity of fluid in mainstream	(8)
ξ	Non-dimensional distance from wall	(3)
ρ	Fluid density	(1)
ρ_G	Value of ρ in mainstream	(5)
τ	Shear stress in fluid	(1)

Subscript

G	Appertaining to conditions in the mainstream

References/

References

No.	Author(s)	Title, etc.
1	P. Bradshaw and D. H. Ferriss	The response of a retarded equilibrium turbulent boundary layer to the sudden removal of pressure gradient. A.R.C.26 758, March, 1965.
2	L. Prandtl	Bericht über Untersuchungen zur ausgebildeten Turbulenz. ZAMM 5, pp.136-139, 1925.
3	M. P. Escudier	The distribution of the mixing length in turbulent flows near walls. Mech. Eng. Dept. Imperial College, TWF/TN/1, 1965.
4	M. P. Escudier, W. B. Nicoll, S. V. Patankar and D. B. Spalding	Unpublished work at Imperial College.
5	J. Rotta	Über die Theorie der turbulenten Grenzschichten Strom. Forsch. Nr.1 (1950). Transl. as "On the theory of the turbulent boundary layer". NACA TM 1344, 1953.
6	E. Truckenbrodt	Ein Quadraturverfahren zur Berechnung der laminaren und turbulenten Reiburg-Schicht bei ebener und rotations symmetrischer Strömung. Ing.-Arch. 20, pp.211-228, 1952.
7	P. S. Klebanoff	Characteristics of turbulence in a boundary layer with zero pressure gradient. NACA Rep.1247, 1955.
8	H. L. Moses	The behaviour of turbulent boundary layers in adverse pressure gradients. MIT GTL Rep. No.73, 1964.
9	B. G. Newman	Some contributions to the study of the turbulent boundary layer near separation. ARCC Rep. ACA-53, 1951.
10	V. A. Sandborn and R. J. Slogar	Study of the momentum distribution of turbulent boundary layers in adverse pressure gradients. NACA TN 3264, 1955.
11	G. B. Schubauer and P. S. Klebanoff	Investigation of separation of the turbulent boundary layer. NACA Rep.1030, 1951.

12/

No.	Author(s)	Title, etc.
12	H. Ludwieg and W. Tillman	Untersuchungen über die Wandschubspannung in Turbulenten Reibungsschichten. Ing.-Arch. 17, pp.288-299, (1949). Transl. as "Investigations of the wall shearing stress in turbulent boundary layers". A.R.C.14 800, April, 1952.
13	W. B. Nicoll and M. P. Escudier	Empirical relationships between the shape factors H_{32} and H_{12} for uniform-density turbulent boundary layers and wall jets. Mech. Eng. Dept. Imperial College, TWF/TN/3, 1965.
14	B. G. J. Thompson	A critical review of existing methods of calculating the turbulent boundary layer. A.R.C. R. & M.3447, August, 1964.
15	P. S. Klebanoff and Z. W. Diehl	Some features of artificially thickened fully developed turbulent boundary layers with zero pressure gradient. NACA Rep.1110, 1952.
16	G. G. Brebner and J. A. Bagley	Pressure and boundary-layer measurements on a two-dimensional wing at low speed. A.R.C. R. & M.2886, February, 1952.
17	F. H. Clauser	Turbulent boundary layers in adverse pressure gradients. J. Aero. Sci. 21, pp.91-108, 1954.
18	A. E. von Doenhoff and N. Tetervin	Determination of general relations for the behaviour of turbulent boundary layers. NACA Rep.772, 1943.
19	A. Fage	Profile and skin-friction aerofoil drags. A.R.C. R. & M.1852, April, 1938.
20	D. E. Gault	Boundary-layer and stalling characteristics of the NACA 63-009 airfoil section. NACA TN 1894, 1949.
21	H. J. Herring and J. F. Norbury	Some experiments on equilibrium turbulent boundary layers in favourable pressure gradients. Princeton University, Dept. Aerospace and Mech. Sci. FLD No.15, 1963.

22/

No.	Author(s)	Title, etc.
22	G. B. Schubauer and P. S. Klebanoff	Investigation of separation of the turbulent boundary layer. NACA Rep.1030, 1951.
23	G. B. Schubauer and W. Spangenberg	Forced mixing in boundary layers. J. Fluid Mech., 8, (1), pp.10-32, 1960.
24	F. Schultz-Grunow	Neues Reibungswiderstandsgezetz für glatte Platten. Luftfahrtforschung, 17, pp.239-246, (1940). Transl. as "New frictional resistance law for smooth plates". NACA TM 986, 1941.

Description/

Description of Figures

Fig. 1. Experimental mixing-length profiles for various turbulent boundary layers. $\lambda \equiv \ell/y_G$, $\xi \equiv y/y_G$; $\ell \equiv$ Prandtl mixing length; $y_G \equiv$ boundary-layer thickness.

(a) Bradshaw and Ferriss[1] 1: Equilibrium boundary layer.

(b) Bradshaw and Ferriss[2] 2: Boundary layer recovering from adverse pressure gradient.

(c) Klebanoff[7]: Flat-plate boundary layer.

(d) Moses[8]: Axisymmetric boundary layer along a horizontal cylinder, adverse pressure gradient.

(e) Newman[9] 1: Boundary layer on rear-stalling aerofoil.

(f) Newman[9] 2: Boundary layer on rear-stalling aerofoil.

Fig.2. Experimental data for the dissipation integral $\bar{s}$ related to the local drag coefficient $\frac{c_f}{2}$ and to the shape factor H.

Fig.3. Experimental data for the relation between the shape factors H_3 and H.

Fig.4. Comparison of measured shape factors with the predictions (curves) made by the method described in the text.

Bradshaw and Ferriss[1] 1: Equilibrium boundary layer.

Bradshaw and Ferriss[1] 2: Boundary layer recovering from adverse pressure gradient.

Brebner and Bagley[16] 1: Symmetrical wing RAE 101, $\alpha = 0°$.

Brebner and Bagley[16] 2: Symmetrical wing RAE 101, $\alpha = 4{\cdot}09°$.

Brebner and Bagley[16] 3: Symmetrical wing RAE 101, $\alpha = 8{\cdot}18°$.

Clauser[17] 1: Equilibrium boundary layer, pressure distribution 1.

Clauser[17] 2: Equilibrium boundary layer, pressure distribution 2.

von Doenhoff and Tetervin[18] 1: Aerofoil NACA 65 (216) - 222 (approx.), $R = 0{\cdot}92 \times 10^6$, $\alpha = 8{\cdot}1°$.

von Doenhoff and Tetervin[18] 2: Aerofoil NACA 65 (216) - 222 (approx.), $R = 2{\cdot}67 \times 10^6$, $\alpha = 8{\cdot}1°$.

von Doenhoff and Tetervin[18] 3: Aerofoil NACA 65 (216) - 222 (approx.), $R = 2{\cdot}64 \times 10^6$, $\alpha = 10{\cdot}1°$.

von Doenhoff and Tetervin[18] 4: Aerofoil NACA nose-opening shape 13, $R = 4{\cdot}18 \times 10^6$, $\alpha = 9{\cdot}1°$.

Fage[19] 1: Joukowski aerofoil, $R = 1{\cdot}665 \times 10^6$.

Fage[19] 2: Joukowski aerofoil, $R = 1{\cdot}248 \times 10^6$.

Gault[20] 1: Aerofoil NACA 63-009, $\alpha = 0°$.

Gault[20] 2: Aerofoil NACA 63-009, $\alpha = 4°$.

Gault[20] 3: Aerofoil NACA 63-009, $\alpha = 6°$.

Gault[20] 4: Aerofoil NACA 63-009, $\alpha = 8{\cdot}5°$.

Herring and Norbury[21]: Equilibrium boundary layer, $\beta \approx -0{\cdot}35$.

Klebanoff and Diehl[15] 1: Flat-plate boundary layer, natural transition.

Klebanoff and Diehl[15] 2: Flat-plate boundary layer recovering from 0·04 in. rod disturbance.

Klebanoff and Diehl[15] 3: Flat-plate boundary layer recovering from 0·25 in. rod disturbance.

Klebanoff and Diehl[15] 4: Flat-plate boundary layer recovering from mesh-screen disturbance.

Klebanoff and Diehl[15] 5: Flat-plate boundary layer recovering from sandpaper-strip disturbance, $u_G = 35$ ft/s.

Klebanoff and Diehl[15] 6: Flat-plate boundary layer recovering from sandpaper-strip disturbance, $u_G = 55$ ft/s.

Klebanoff and Diehl[15] 7: Flat-plate boundary layer recovering from sandpaper-strip disturbance, $u_G = 108$ ft/s.

Ludwieg and Tillmann[12] A: Moderate adverse pressure gradient.

Ludwieg and Tillmann[12] B: High adverse pressure gradient.

Ludwieg and Tillmann[12] C: Favourable pressure gradient.

Ludwieg and Tillman[1] (unpublished) : Adverse pressure gradient.

Ludwieg and Tillman[2] (unpublished) : Adverse pressure gradient.

Ludwieg and Tillman[3] (unpublished) : Adverse pressure gradient.

Ludwieg and Tillmann[4] (unpublished) : Adverse pressure gradient.

Moses[8] 1: Axisymmetric boundary layer along horizontal cylinder, adverse pressure gradient.

Moses[8] 2: Axisymmetric boundary layer along horizontal cylinder, adverse pressure gradient.

Moses[8] 3: Axisymmetric boundary layer along horizontal cylinder, adverse pressure gradient.

Moses[8] 4: Axisymmetric boundary layer along horizontal cylinder, adverse pressure gradient.

Moses[8] 5: Axisymmetric boundary layer along horizontal cylinder, adverse pressure gradient followed by near-zero favourable pressure gradient.

Moses/

Moses[8] 6: Axisymmetric boundary layer along horizontal cylinder, adverse pressure gradient followed by near-zero pressure gradient.

Newman[9]: Symmetrical rear-stalling aerofoil.

Sandborn and Slogar[10] : Adverse pressure gradient.

Schubauer and Klebanoff[11]: Convex wall, adverse pressure gradient.

Schubauer and Spangenberg[23] A: Moderate adverse pressure gradient.

Schubauer and Spangenverg[23] B: Adverse pressure gradient.

Schubauer and Spangenberg[23] C: Moderate adverse pressure gradient.

Schubauer and Spangenberg[23] D: Adverse pressure gradient.

Schubauer and Spangenberg[23] E: Adverse pressure gradient.

Schubauer and Spangenberg[23] F: Adverse pressure gradient.

Schultz-Grunow[24]: Flat-plate boundary layer.

SJ

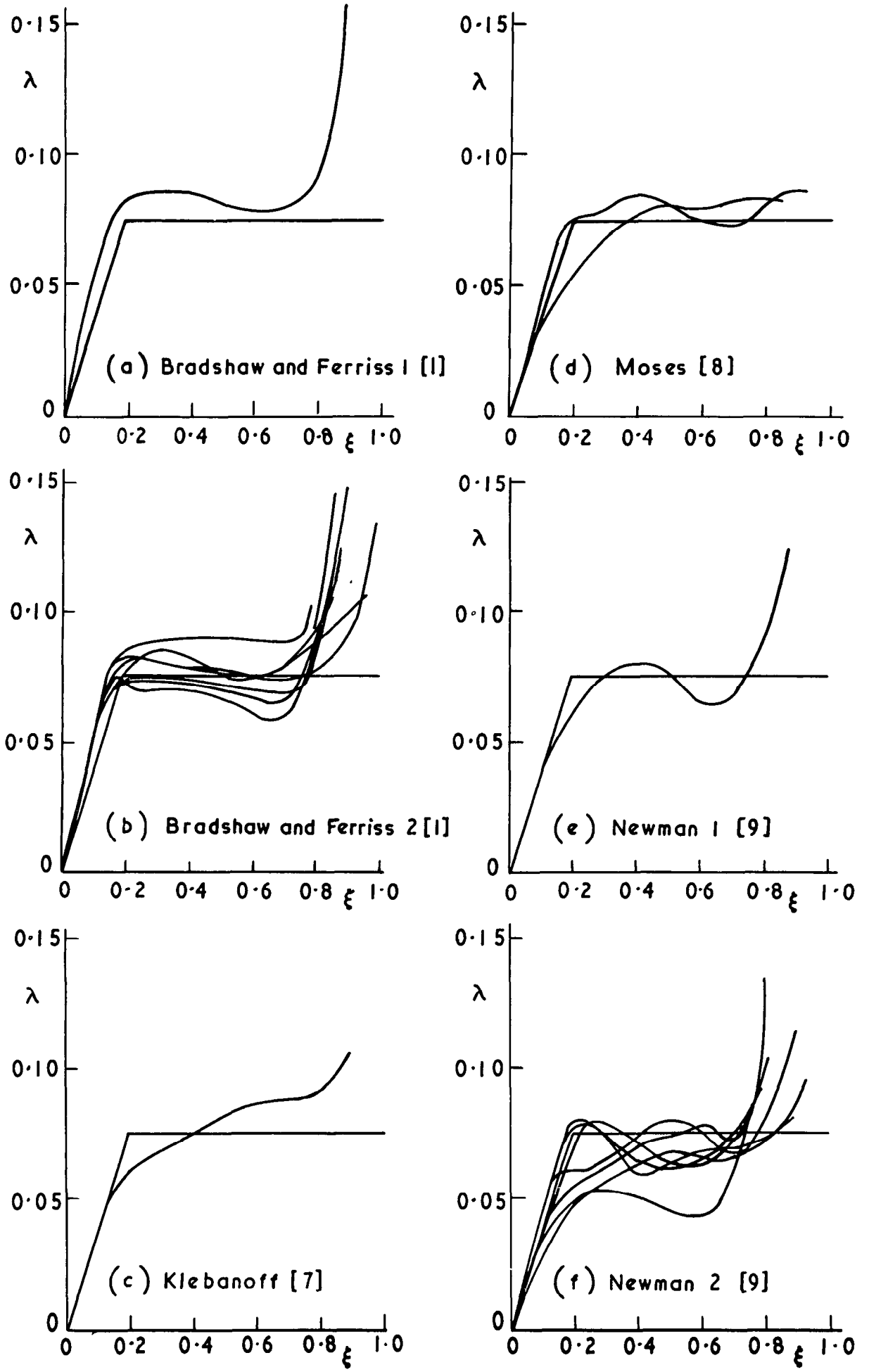

FIG.1 Experimental mixing-length profiles for various turbulent boundary layers. $\lambda \equiv l/y_G$, $\xi \equiv y/y_G$; $l \equiv$ Prandtl mixing length; $y_G =$ boundary-layer thickness

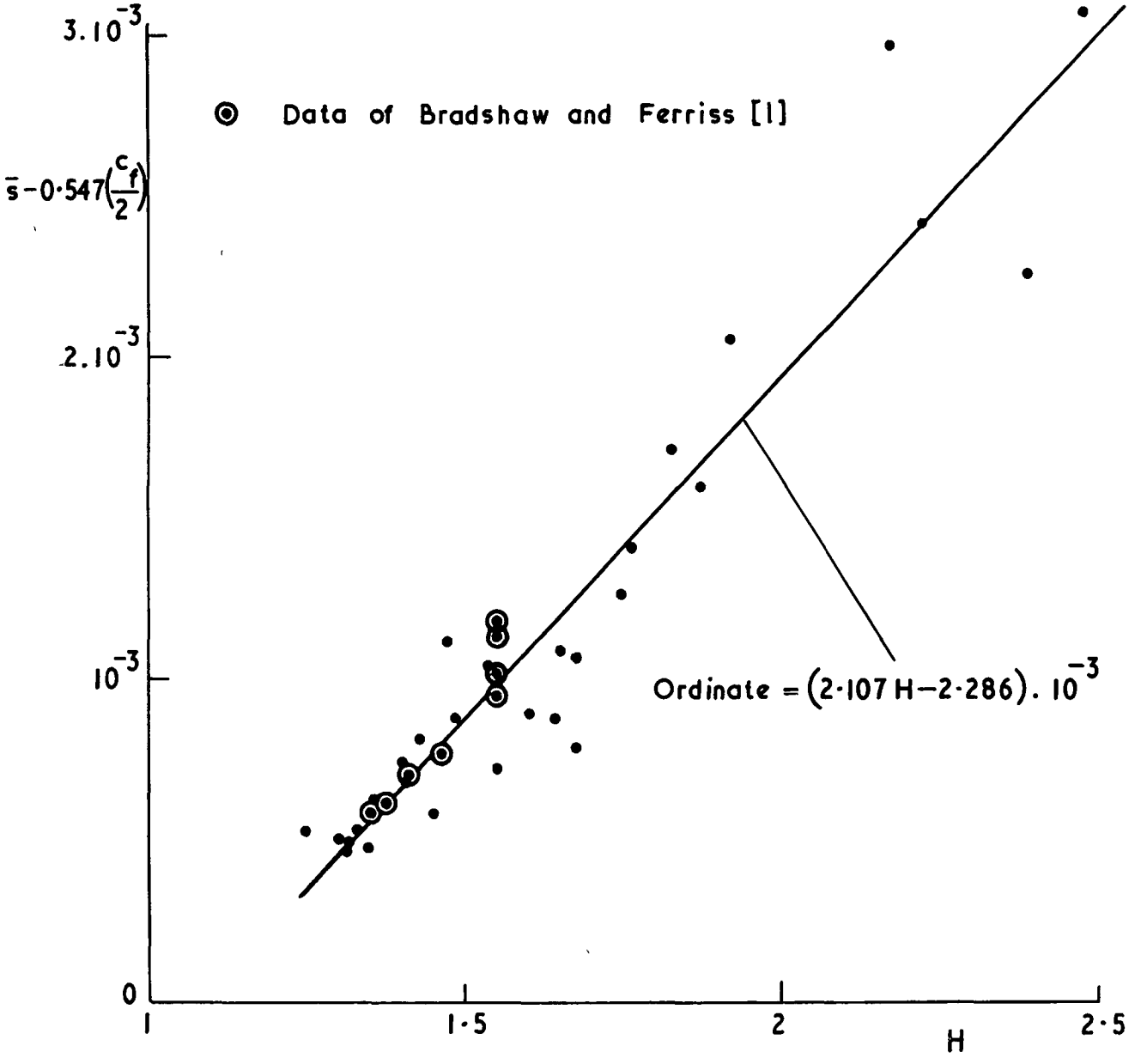

FIG. 2 Experimental data for the dissipation integral $\bar{s}$, related to the local drag coefficient $c_f/2$ and to the shape factor H

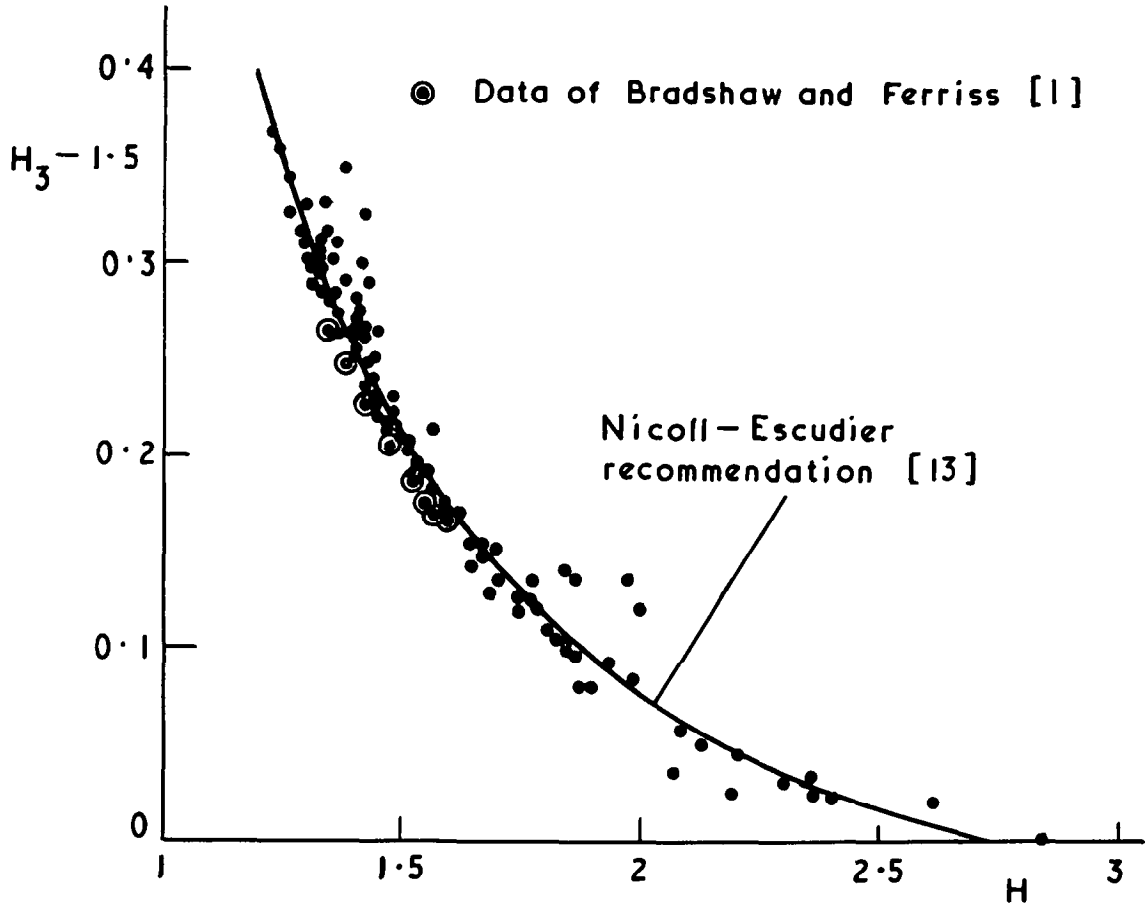

FIG. 3 Experimental data for the relation between the shape factors H_3 and H

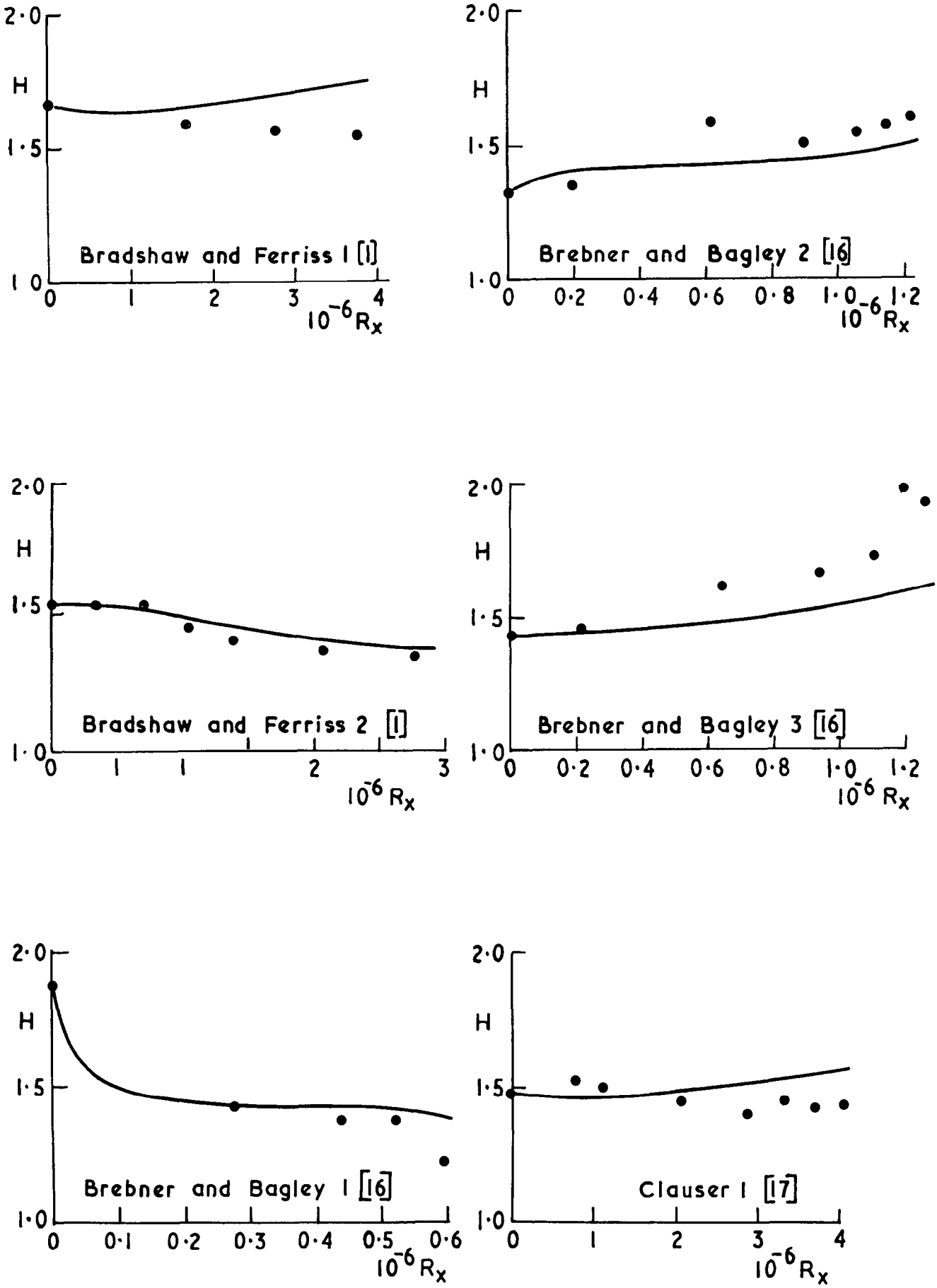

FIG. 4: Comparison of measured shape factors with the predictions (curves) made by the method described in the text

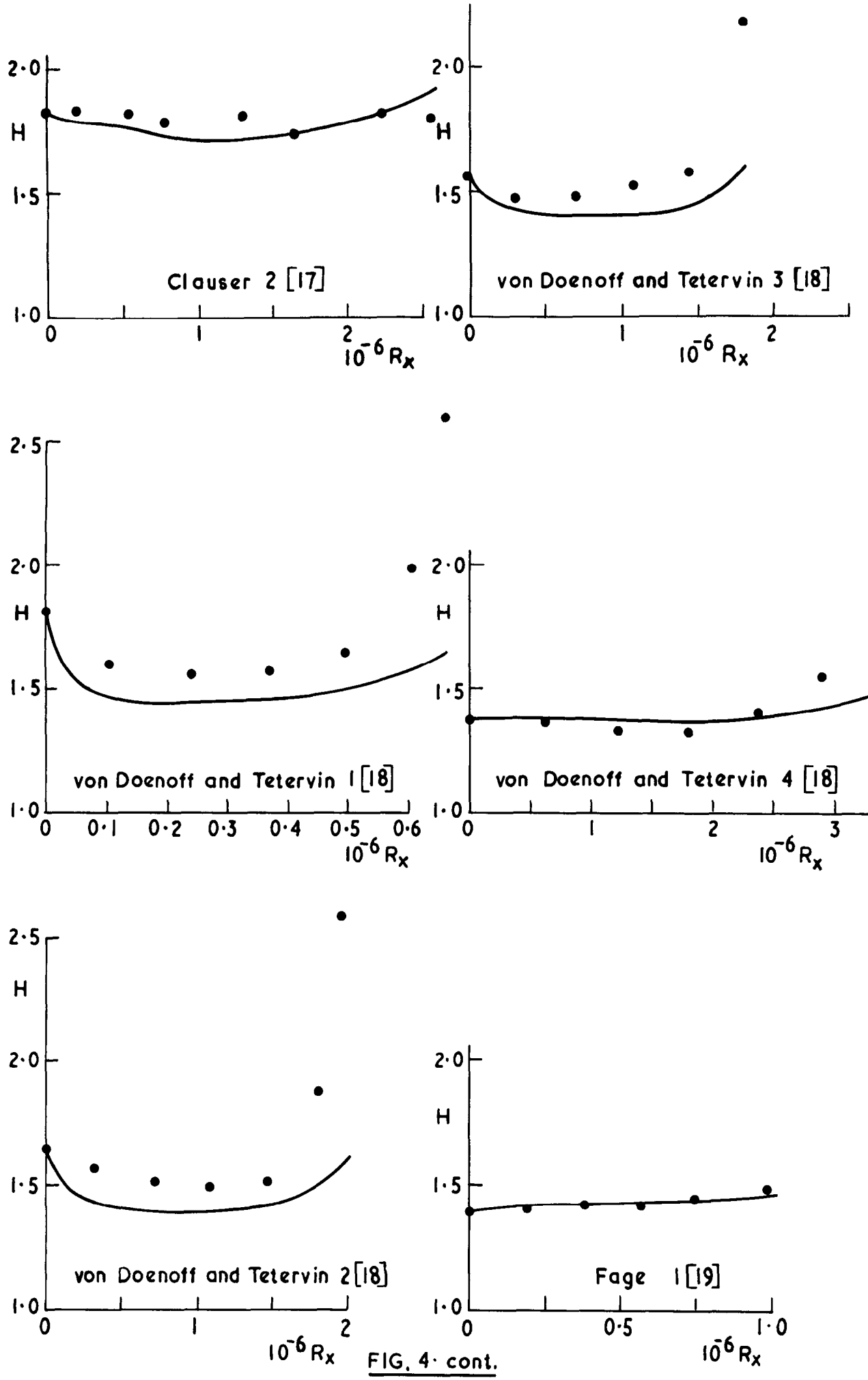
2·0
H
1·5
1·0
Clauser 2 [17]
0
1
2
10⁻⁶ Rx
2·0
H
1·5
1·0
von Doenoff and Tetervin 3 [18]
0
1
2
10⁻⁶ Rx
2·5
2·0
H
1·5
1·0
von Doenoff and Tetervin 1 [18]
0
0·1
0·2
0·3
0·4
0·5
0·6
10⁻⁶ Rx
2·0
H
1·5
1·0
von Doenoff and Tetervin 4 [18]
0
1
2
3
10⁻⁶ Rx
2·5
H
2·0
1·5
1·0
von Doenoff and Tetervin 2 [18]
0
1
2
10⁻⁶ Rx
2·0
H
1·5
1·0
Fage 1 [19]
0
0·5
1·0
10⁻⁶ Rx

FIG. 4· cont.

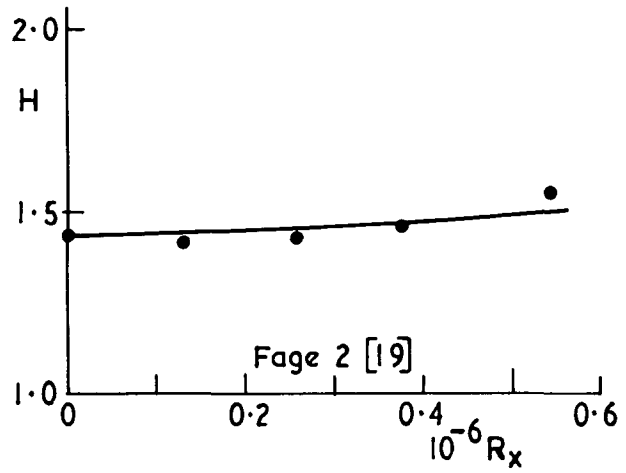
2·0
H
1·5
1·0
Fage 2 [19]
0
0·2
0·4
0·6
$10^{-6}R_x$

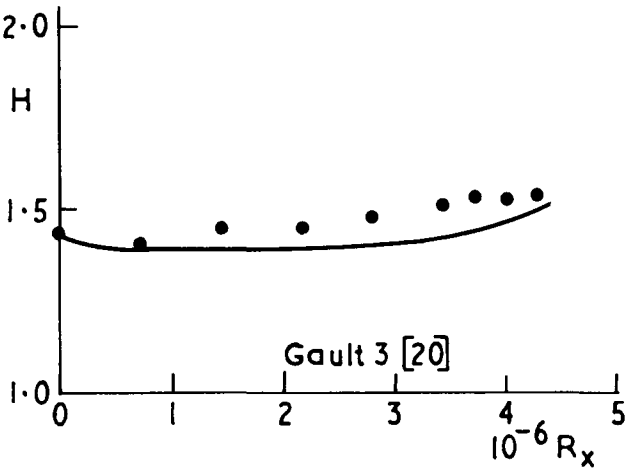
2·0
H
1·5
1·0
Gault 3 [20]
0
1
2
3
4
5
$10^{-6}R_x$

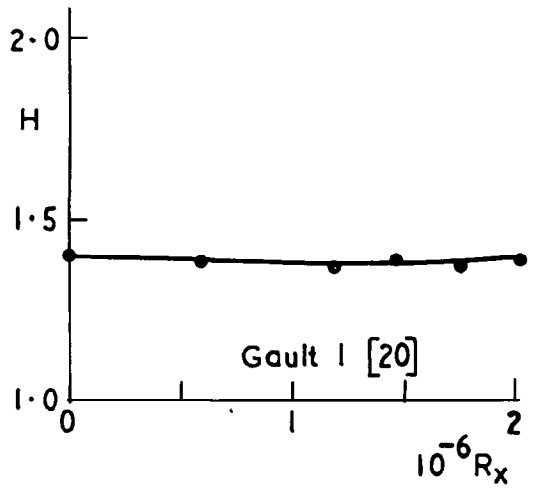
2·0
H
1·5
1·0
Gault 1 [20]
0
1
2
$10^{-6}R_x$

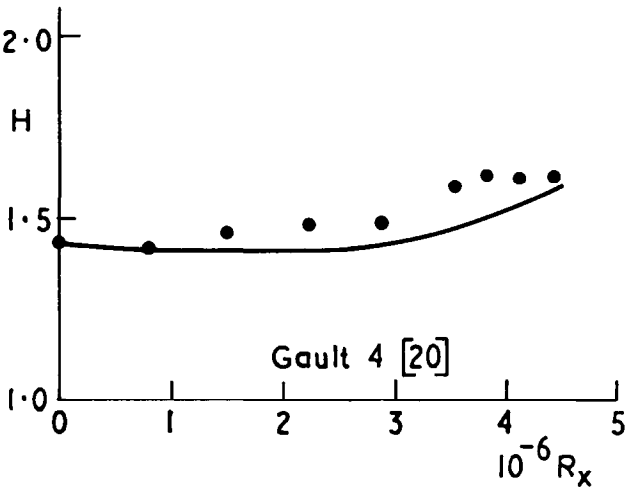
2·0
H
1·5
1·0
Gault 4 [20]
0
1
2
3
4
5
$10^{-6}R_x$

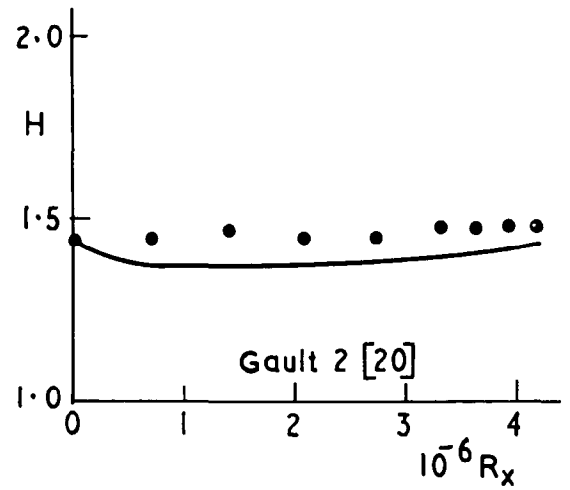
2·0
H
1·5
1·0
Gault 2 [20]
0
1
2
3
4
$10^{-6}R_x$

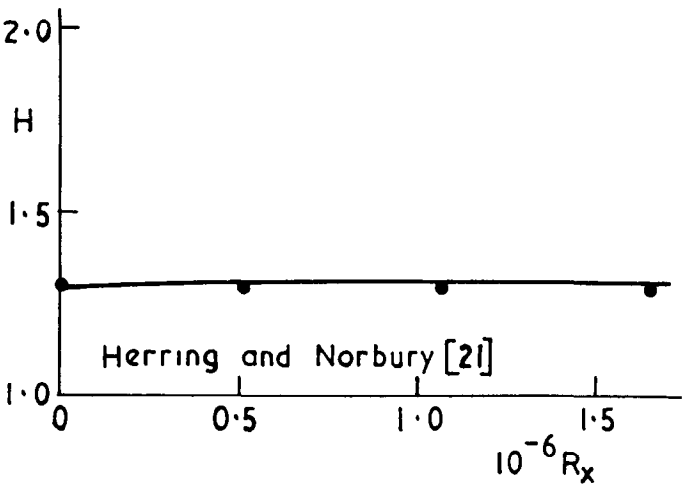
2·0
H
1·5
1·0
Herring and Norbury [21]
0
0·5
1·0
1·5
$10^{-6}R_x$

FIG. 4 cont.

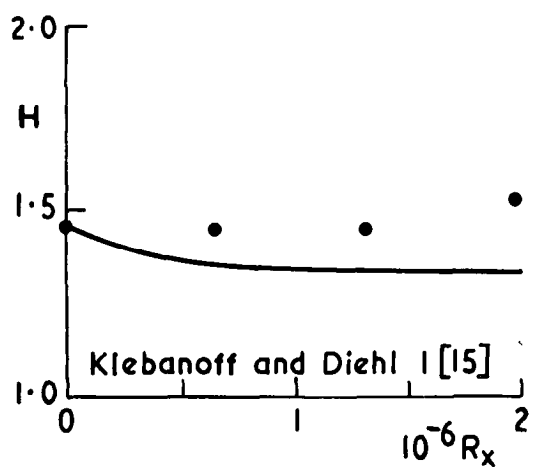
2·0
H
1·5
1·0
Klebanoff and Diehl 1 [15]
0
1
2
$10^{-6}R_x$

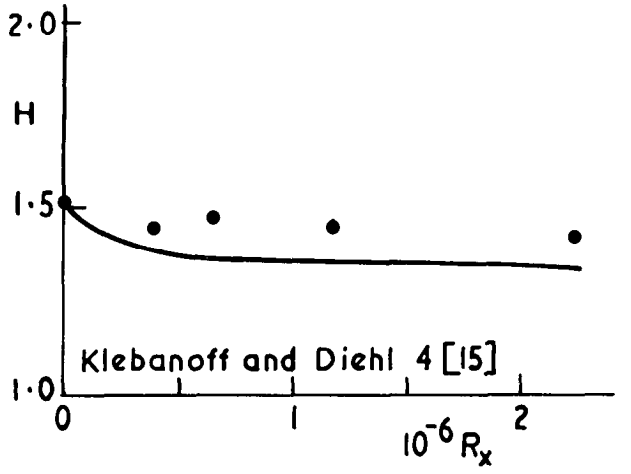
2·0
H
1·5
1·0
Klebanoff and Diehl 4 [15]
0
1
2
$10^{-6}R_x$

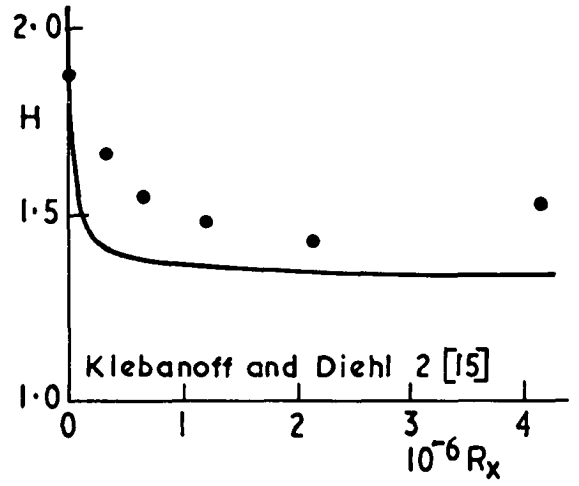
2·0
H
1·5
1·0
Klebanoff and Diehl 2 [15]
0
1
2
3
4
$10^{-6}R_x$

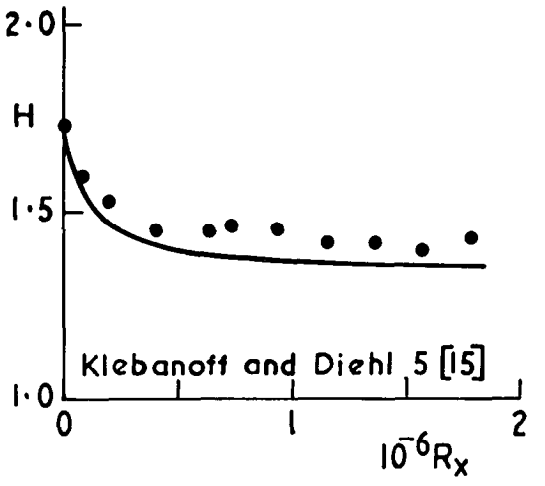
2·0
H
1·5
1·0
Klebanoff and Diehl 5 [15]
0
1
2
$10^{-6}R_x$

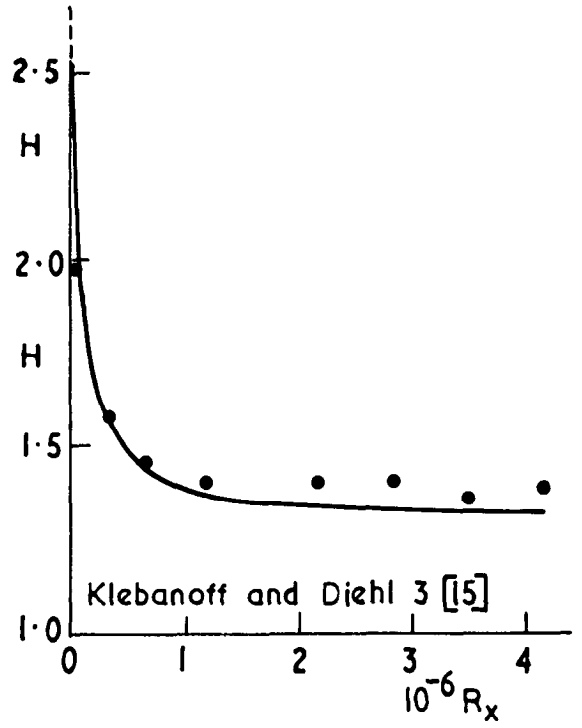
2·5
H
2·0
H
1·5
1·0
Klebanoff and Diehl 3 [15]
0
1
2
3
4
$10^{-6}R_x$

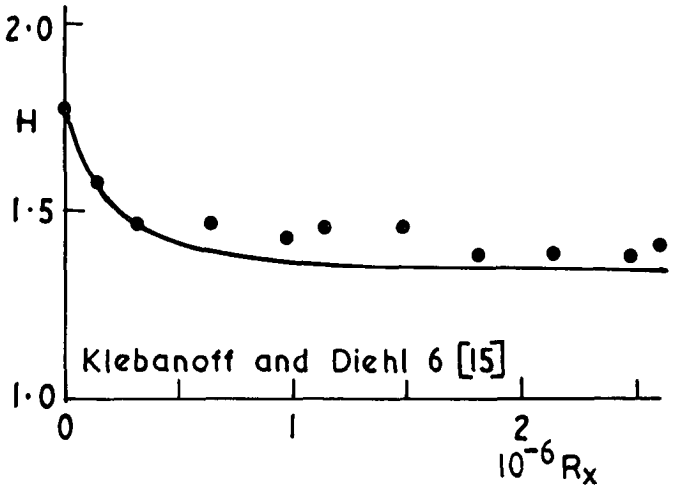
2·0
H
1·5
1·0
Klebanoff and Diehl 6 [15]
0
1
2
$10^{-6}R_x$

FIG. 4 cont.

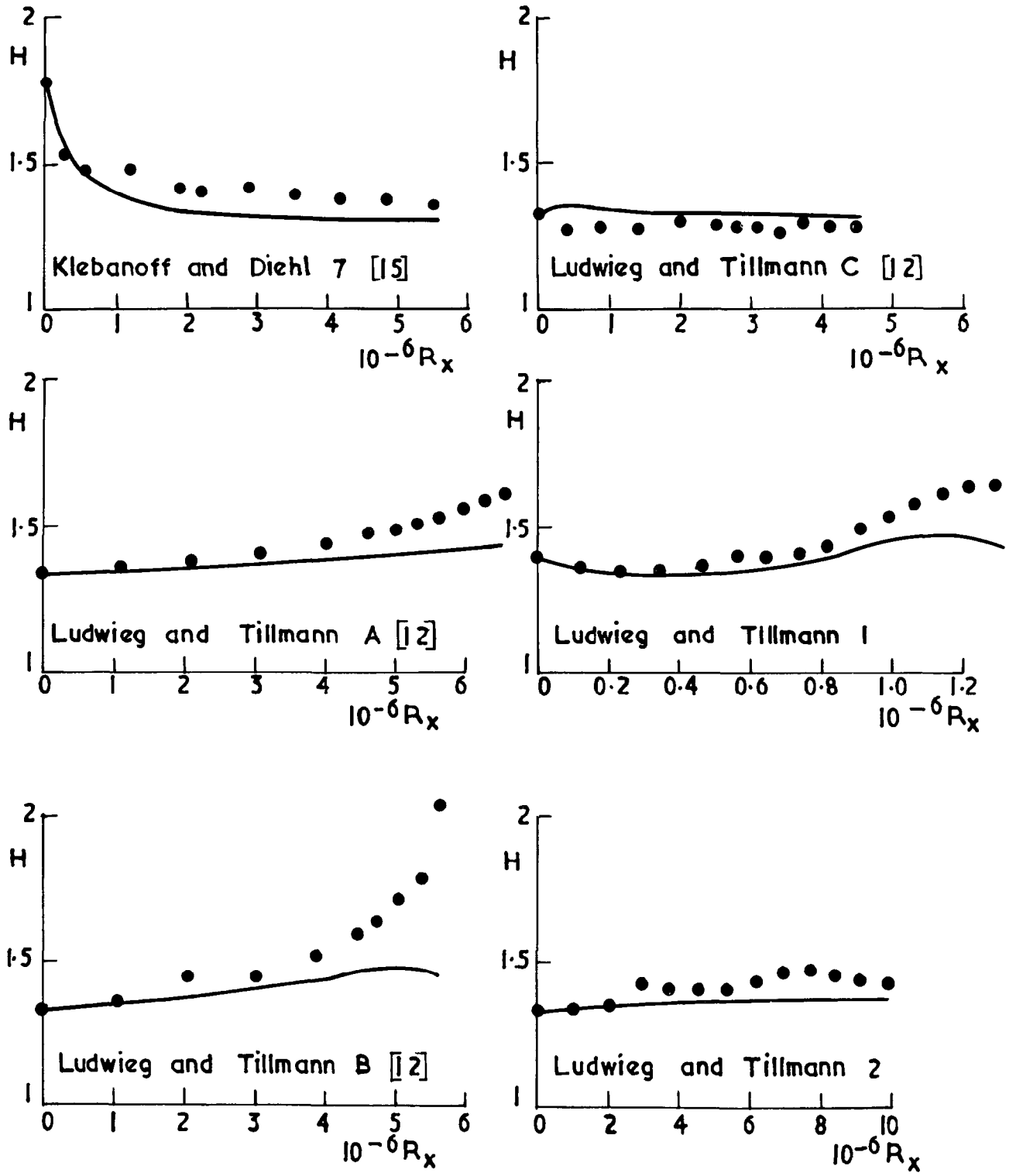
Klebanoff and Diehl 7 [15]
Ludwieg and Tillmann C [12]
Ludwieg and Tillmann A [12]
Ludwieg and Tillmann I
Ludwieg and Tillmann B [12]
Ludwieg and Tillmann 2
H
$10^{-6}R_x$

FIG. 4. cont.

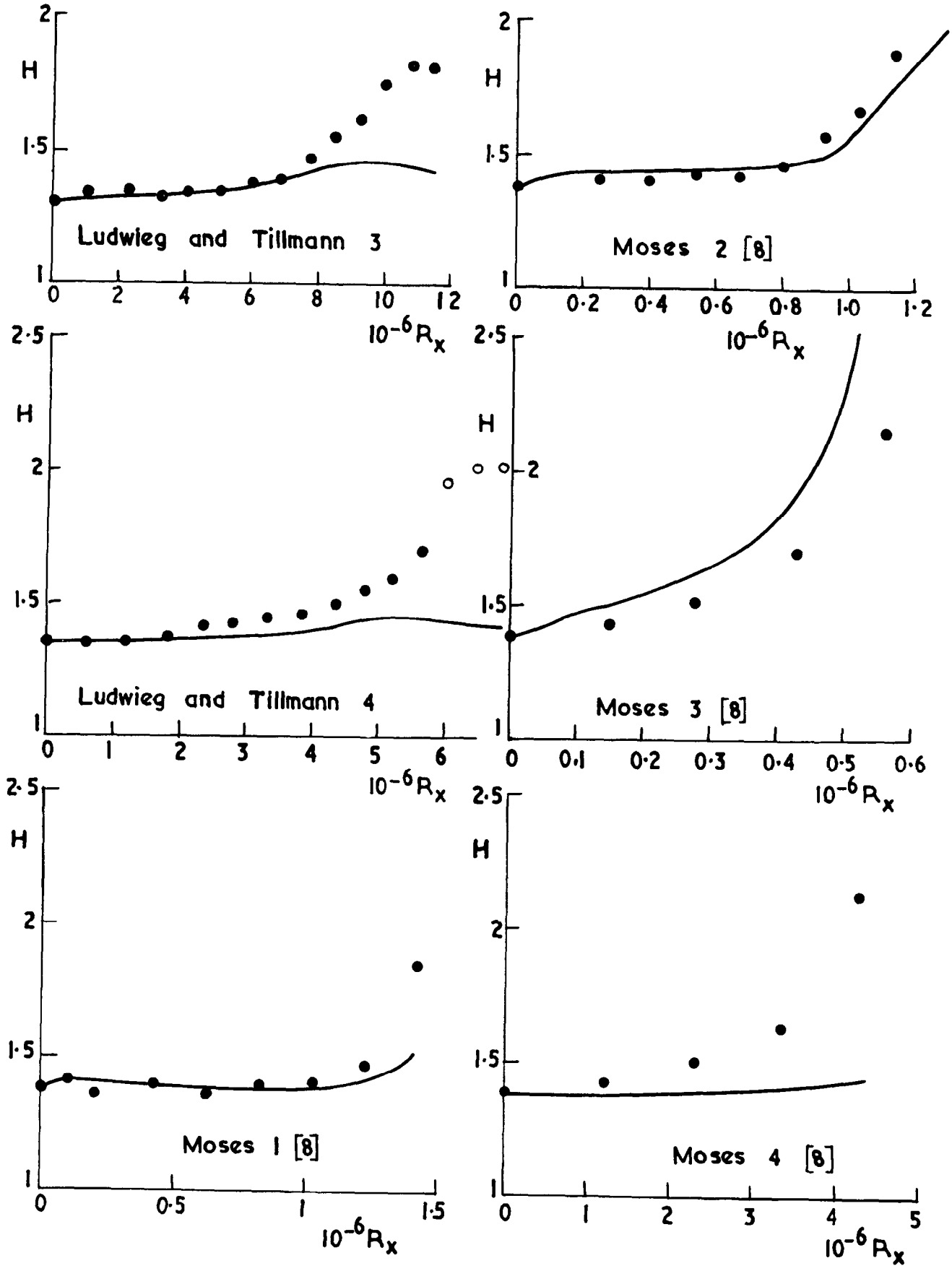
H
Ludwieg and Tillmann 3
$10^{-6}R_x$
Moses 2 [8]
Ludwieg and Tillmann 4
Moses 3 [8]
Moses 1 [8]
Moses 4 [8]

FIG.4 cont.

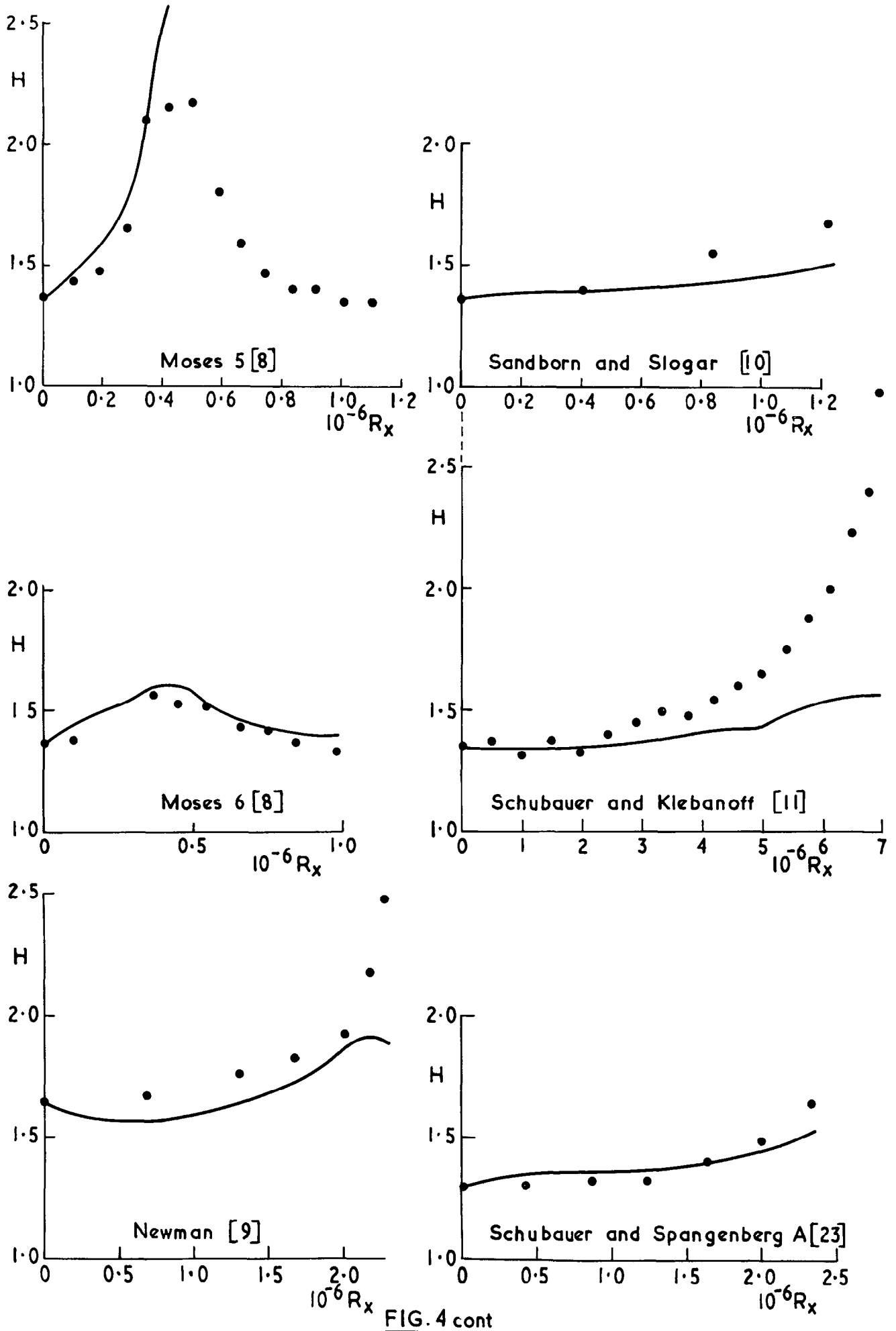
2·5
H
2·0
1·5
1·0
0
0·2
0·4
0·6
0·8
1·0
1·2
$10^{-6}R_x$
Moses 5 [8]
Sandborn and Slogar [10]
Moses 6 [8]
Schubauer and Klebanoff [11]
1
2
3
4
5
6
7
0·5
Newman [9]
Schubauer and Spangenberg A[23]
2·5

FIG. 4 cont

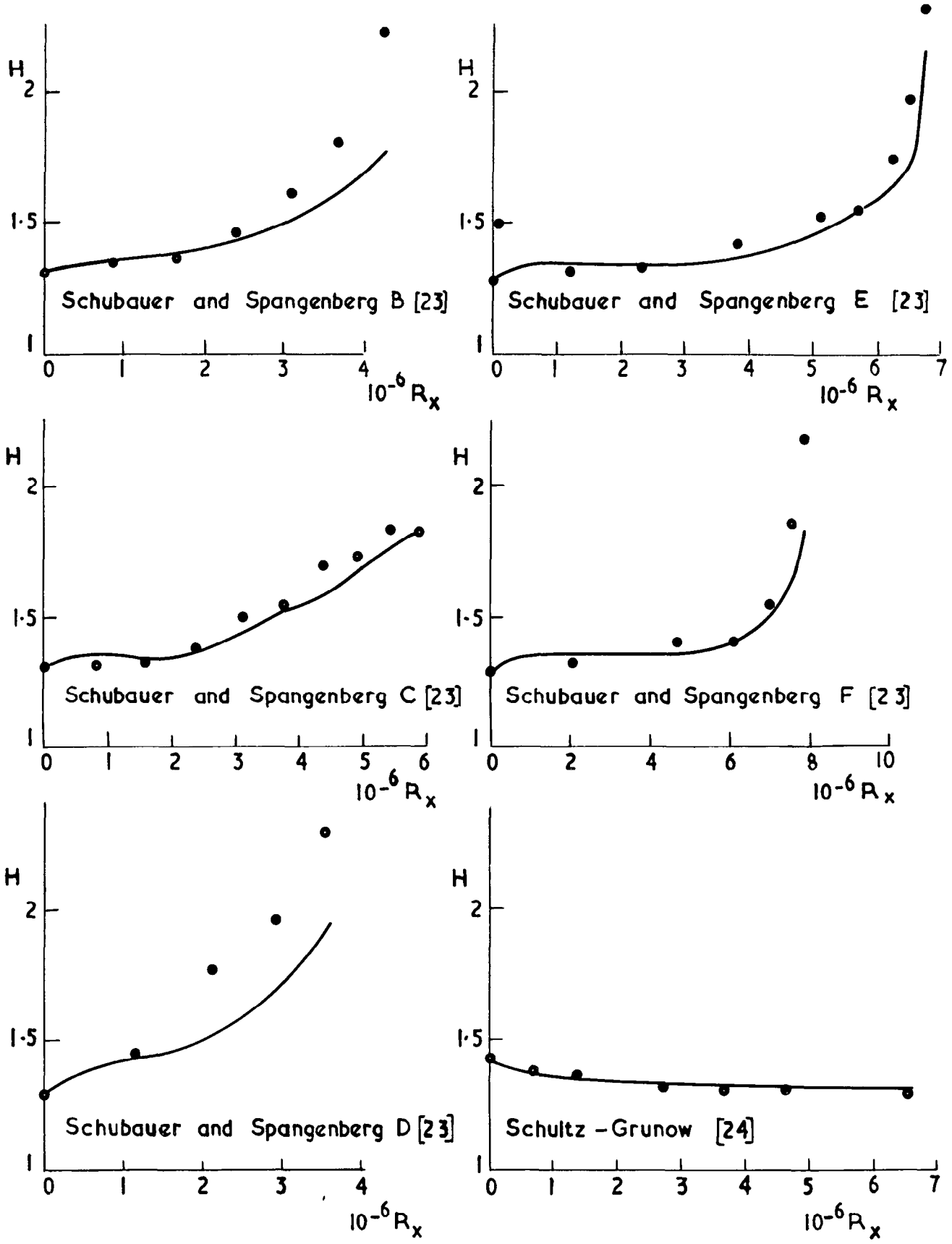
H
2
1·5
1
0 1 2 3 4
10⁻⁶ Rx
Schubauer and Spangenberg B [23]
0 1 2 3 4 5 6 7
Schubauer and Spangenberg E [23]
0 1 2 3 4 5 6
Schubauer and Spangenberg C [23]
0 2 4 6 8 10
Schubauer and Spangenberg F [23]
Schubauer and Spangenberg D [23]
Schultz - Grunow [24]

FIG.4. conc.

A.R.C. C.P. No.875
August, 1965
Escudier, M. P. and Spalding, D. B.

A NOTE ON THE TURBULENT UNIFORM-PROPERTY HYDRODYNAMIC BOUNDARY LAYER ON A SMOOTH IMPERMEABLE WALL; COMPARISONS OF THEORY WITH EXPERIMENT

The recent experimental data of Bradshaw and Ferriss[1] are compared with generalisations deduced from earlier data, in respect of the mixing-length distribution and the dissipation integral; the agreement is satisfactory.

Also presented is a preliminary theory of boundary-layer development employing an empirical formula for the relation between the dissipation integral, the drag coefficient and the shape factor; the integral momentum and kinetic-energy equations are solved numerically. The predictions of this theory are compared, in respect of shape factor, with the experiments of Bradshaw and Ferriss and those of many other experimenters. The agreement is satisfactory except for large adverse pressure gradient, where divergences of both positive and negative sign are observed; the reasons for these divergences are discussed.

A.R.C. C.P. No.875
August, 1965
Escudier, M. P. and Spalding, D. B.

A NOTE ON THE TURBULENT UNIFORM-PROPERTY HYDRODYNAMIC BOUNDARY LAYER ON A SMOOTH IMPERMEABLE WALL; COMPARISONS OF THEORY WITH EXPERIMENT

The recent experimental data of Bradshaw and Ferriss[1] are compared with generalisations deduced from earlier data, in respect of the mixing-length distribution and the dissipation integral; the agreement is satisfactory.

Also presented is a preliminary theory of boundary-layer development employing an empirical formula for the relation between the dissipation integral, the drag coefficient and the shape factor; the integral momentum and kinetic-energy equations are solved numerically. The predictions of this theory are compared, in respect of shape factor, with the experiments of Bradshaw and Ferriss and those of many other experimenters. The agreement is satisfactory except for large adverse pressure gradient, where divergences of both positive and negative sign are observed; the reasons for these divergences are discussed.

A.R.C. C.P. No.875
August, 1965
Escudier, M. P. and Spalding, D. B.

A NOTE ON THE TURBULENT UNIFORM-PROPERTY HYDRODYNAMIC BOUNDARY LAYER ON A SMOOTH IMPERMEABLE WALL; COMPARISONS OF THEORY WITH EXPERIMENT

The recent experimental data of Bradshaw and Ferriss[1] are compared with generalisations deduced from earlier data, in respect of the mixing-length distribution and the dissipation integral; the agreement is satisfactory.

Also presented is a preliminary theory of boundary-layer development employing an empirical formula for the relation between the dissipation integral, the drag coefficient and the shape factor; the integral momentum and kinetic-energy equations are solved numerically. The predictions of this theory are compared, in respect of shape factor, with the experiments of Bradshaw and Ferriss and those of many other experimenters. The agreement is satisfactory except for large adverse pressure gradient, where divergences of both positive and negative sign are observed; the reasons for these divergences are discussed.

DETACHABLE ABSTRACT CARDS

Printed and published by

HER MAJESTY'S STATIONERY OFFICE

To be purchased from
49 High Holborn, London W C 1
423 Oxford Street, London W 1
13A Castle Street, Edinburgh 2
109 St. Mary Street, Cardiff
Brazennose Street, Manchester 2
50 Fairfax Street, Bristol 1
35 Smallbrook, Ringway, Birmingham 5
80 Chichester Street, Belfast 1
or through any bookseller

Printed in England

C.P. No. 875

S O Code No 23-9016-75